HHS Public Access

Author manuscript

*Cell Calcium*. Author manuscript; available in PMC 2015 April 27.

Published in final edited form as:

*Cell Calcium*. 2013 November ; 54(5): 350–361. doi:10.1016/j.ceca.2013.08.004.

# Calcium homeostasis in *Pseudomonas aeruginosa* requires multiple transporters and modulates swarming motility

**Manita Guragain**, **Dirk L. Lenaburg**, **Frank S. Moore**, **Ian Reutlinger**, and **Marianna A. Patrauchan***

Department of Microbiology and Molecular Genetics, Oklahoma State University, Stillwater, OK

## Abstract

*Pseudomonas aeruginosa* is an opportunistic human pathogen causing severe acute and chronic infections. Earlier we have shown that calcium ($Ca^{2+}$) induces *P. aeruginosa* biofilm formation and production of virulence factors. To enable further studies of the regulatory role of $Ca^{2+}$, we characterized $Ca^{2+}$ homeostasis in *P. aeruginosa* PAO1 cells. By using $Ca^{2+}$-binding photoprotein aequorin, we determined that the concentration of free intracellular $Ca^{2+}$ ($[Ca^{2+}]_{in}$) is 0.14±0.05 μM. In response to external $Ca^{2+}$, the $[Ca^{2+}]_{in}$ quickly increased at least 13 fold followed by a multi-phase decline by up to 73%. Growth at elevated $Ca^{2+}$ modulated this response. Treatment with inhibitors known to affect $Ca^{2+}$ channels, monovalent cations gradient, or P-type and F-type ATPases impaired $[Ca^{2+}]_{in}$ response, suggesting the importance of the corresponding mechanisms in $Ca^{2+}$ homeostasis. To identify $Ca^{2+}$ transporters maintaining this homeostasis, bioinformatic and LC-MS/MS-based membrane proteomic analyses were used. $[Ca^{2+}]_{in}$ homeostasis was monitored for seven $Ca^{2+}$-affected and eleven bioinformatically predicted transporters by using transposon insertion mutants. Disruption of P-type ATPases PA2435, PA3920, and ion exchanger PA2092 significantly impaired $Ca^{2+}$ homeostasis. The lack of PA3920 and vanadate treatment abolished $Ca^{2+}$- induced swarming, suggesting the role of the P-type ATPase in regulating *P. aeruginosa* response to $Ca^{2+}$.

### Keywords

Calcium homeostasis; ATPase; Ion exchanger; Aequorin; Calcium transporters

## INTRODUCTION

Calcium ($Ca^{2+}$) is a well-known signaling molecule that regulates a number of essential processes in eukaryotes [1]. Abnormalities in cellular $Ca^{2+}$ homeostasis have been implicated in many human diseases, including diseases associated with bacterial infections,



*Corresponding author: Marianna A. Patrauchan Dept. of Microbiology and Molecular Genetics Oklahoma State University, 307 LSE Stillwater, OK, 74075 Tel: (405) 744-8148 Fax: (405) 744-6790 m.patrauchan@okstate.edu.

for example, cystic fibrosis (CF) and endocarditis. In addition, $Ca^{2+}$ plays a regulatory role in innate immune response [2], and its intracellular ($[Ca^{2+}]_{in}$) and extracellular ($[Ca^{2+}]_{ex}$) concentrations fluctuate in response to inflammation. For example, the levels of $[Ca^{2+}]$ in pulmonary fluid and nasal secretions of CF patients are increased [3, 4]. Altogether the evidence suggests that cellular $Ca^{2+}$ balance in a host may provide an environmental cue for opportunistic pathogenic bacteria and trigger their virulence. In support, in prokaryotes, $Ca^{2+}$ has been implicated in various physiological processes such as spore formation, motility, cell differentiation, transport, and virulence (reviewed in [5]). It has also been shown that $Ca^{2+}$ modulates bacterial gene expression [6-8], suggesting its regulatory role in prokaryotes. Furthermore, there is growing evidence that $Ca^{2+}$ plays a signaling role in prokaryotes, which requires a tight control of cellular $Ca^{2+}$ homeostasis. Several bacteria including *Escherichia coli* [9], *Propionibacterium acnes* [10], *Streptococcus pneumoniae* [11] *Bacillus subtilis* [12] and cyanobacteria [13] have been shown to maintain intracellular $Ca^{2+}$ at sub-micromolar levels, and produce $Ca^{2+}$ transients in response to environmental and physiological conditions [14, 15]. Such responses may play a key role in $Ca^{2+}$-regulated bacterial physiology and virulence, however, the molecular mechanisms of bacterial $Ca^{2+}$ homeostasis have not been well characterized. Several studies suggest that bacteria control their $[Ca^{2+}]_{in}$ by using multiple mechanisms of transporting or chelating $Ca^{2+}$ (reviewed in [5]).

Three major types of $Ca^{2+}$ transport systems have been described in prokaryotes: gradient driven $Ca^{2+}$ exchangers, ATP-ases, and non-proteinaceous polyhydroxybutyrate-polyphosphates (PHB-PP) channels. $Ca^{2+}$ exchangers have been identified in a number of bacterial genera and are thought to serve as a major mechanism for $Ca^{2+}$ transport in prokaryotes [16]. They are low-affinity $Ca^{2+}$ transporters that use the energy stored in the electrochemical gradient of ions, and, depending on the gradient, can operate in both directions. The specificity of the transporters may vary. For example, YftkE (ChaA) from *B. subtilis* [17] as well as ApCAX and SynCAX from cyanobacteria [18] are $Ca^{2+}$- specific, whereas ChaA from *E. coli* exhibits $Na^+/H^+$ and $K^+/H^+$ antiport activity in addition to $Ca^{2+}/H^+$ [19]. $Ca^{2+}$ exchangers may also play role in cell sensitivity to $Ca^{2+}$ and salt tolerance, as exemplified by cyanobacterial ApCAX and SynCAX [18]. ATP-ases are mostly high-affinity pumps that export cations from the cytosol by using the energy of ATP. They include P-type and F-type ATPases. $Ca^{2+}$- translocating P-type ATPases belong to P2A and P2B subgroups, as classified in [20]. The former are similar to mammalian sarco(endo)plasmic reticulum (SERCA) $Ca^{2+}$ pumps exporting $Ca^{2+}$ against steep transmembrane gradients, and the latter are similar to plasma membrane (PMCA) calmodulin-binding ATPases. Five characterized prokaryotic P2A-ATPases include PacL from cyanobacteria [21], LMCA1 from *Listeria monocytogenes* [22], YloB from *Bacillus subtilis* [23], CaxP from *Streptococcus penumoniae* [11], and PacL from *Flavobacterium odoratum* [24]. Most of them were shown to export $Ca^{2+}$ in membrane vesicles and proposed to play a role in cell protection against high $Ca^{2+}$. LMCA1 from *L. monocytogenes* [22] and PacL from *F. odoratum* [21] were shown to undergo $Ca^{2+}$-dependent phosphorylation required to transport $Ca^{2+}$. F-type ATPases, or ATP synthases, are known to synthesize ATP at the expense of transmembrane electrochemical gradient of protons (most commonly). So far, only one F-type ATPase AtpD in *E. coli* was shown to play role in

$Ca^{2+}$ homeostasis, most likely due to its role in ATP synthesis [25]. Overall, although several prokaryotic gradient- and ATP- driven transporters were shown to translocate $Ca^{2+}$ *in-vitro*, only few were tested for their role in cellular $Ca^{2+}$ homeostasis *in-vivo*, of which only ion-exchanger SynCAX in *Synechocystis* sp. PCC6803 was shown to play role in cellular $Ca^{2+}$ efflux [18]. The difficulty of identifying the roles of $Ca^{2+}$ transporters *in-vivo* is likely due to their functional redundancy, the molecular basis of which requires further studies.

*Pseudomonas aeruginosa* is an opportunistic human pathogen, and a major cause of nosocomial infections and severe chronic infections in endocarditis and in CF patients. Earlier, we showed that growth at high $Ca^{2+}$ enhances *P. aeruginosa* biofilm formation and induces biosynthesis of several secreted virulence factors including alginate, extracellular proteases and pyocyanin [6, 7]. However, the molecular mechanisms of $Ca^{2+}$ regulation are not defined. To enable studies required to uncover such mechanisms, it is necessary to first characterize cellular $Ca^{2+}$ homeostasis in this organism. Therefore, the aim of this work was to measure the intracellular $Ca^{2+}$ concentration ($[Ca^{2+}]_{in}$) in *P. aeruginosa* cells and characterize its responses to external $Ca^{2+}$. We employed a recombinant photoprotein aequorin-based reporter system, which has been successfully used to measure $[Ca^{2+}]_{in}$ in live prokaryotic cells [12, 25], and to monitor both short- and long-term $[Ca^{2+}]_{in}$ responses to external $Ca^{2+}$ transients [9, 12] as well as other environmental and physiological determinants [12, 15]. We also aimed to identify $Ca^{2+}$ transporters that play role in maintaining cellular $Ca^{2+}$ homeostasis. The strategy combined bioinformatic and proteomic approaches, followed by characterization of transposon insertion mutants obtained from the University of Washington Genome Center. This study presents the first evidence of $Ca^{2+}$ homeostasis in *P. aeruginosa* and identifies several mechanisms and proteins required for maintaining $Ca^{2+}$ homeostasis and regulating $Ca^{2+}$-induced swarming motility. In addition, the results provide a basis and excellent tools for further studies of the roles of cellular $Ca^{2+}$ homeostasis in the regulation of $Ca^{2+}$-modulated physiology and virulence of this important human pathogen.

## MATERIALS AND METHODS

**Chemicals** used in this study are listed in the supplementary information. Primers were obtained from Integrated DNA Technologies Inc.

### Bacterial strains, plasmids, and media

*P. aeruginosa* strain PAO1, the non-mucoid strain with genome sequence available was used in the study. Biofilm minimal medium (BMM) was made as described in [6]. When required, $CaCl_2.2H_2O$ was added to final concentration of 1 or 5 mM. For proteomic studies, PAO1 cells were first grown in 5 ml tubes for 16 h (mid-log), and then used to inoculate (0.1 %) 100 ml fresh medium in 250 ml flasks. The cultures were grown to mid-log growth phase and harvested by centrifugation. Transposon insertion mutants were obtained from the University of Washington Two - Allele library and are listed in Table 1. The mutants contained either ISphoA/hah or ISlacZ/hah insertions with tetracycline resistance cassette that disrupted the genes of interest. The mutations were confirmed by two-step PCR: first,

transposon flanking primers were used to verify that the target gene is disrupted, and second, transposon-specific primers were used to confirm the transposon insertion. The primer sequence is available at www.gs.washington.edu. For convenience, the mutants were designated as PA:IS, where PA is the identifying number of the disrupted gene from *P. aeruginosa* PAO1 genome (www.pseudomonas.com).

## Sequence analyses

To predict $Ca^{2+}$ transporters in *P. aeruginosa* PAO1 genome, we applied BLASTp sequence alignments, using the National Centre for Biotechnology Information (NCBI) non-redundant database (GenBank release 160.1), as well as functional domains search using Conserved Domain Database (CDD) and PROSITE. Homologous proteins were selected based on at least 25 % identity over the full length of amino acid sequence. For phylogenetic analyses, amino acid sequences of the functionally characterized transporters of $Ca^{2+}$ and other cations were aligned with *P. aeruginosa* putative $Ca^{2+}$ transporters using ClustalW. Thus obtained multiple sequence alignments were then used to build unrooted phylogenetic tree using Neighbor-joining algorithm in the MEGA 5.1 software.

## Proteomic analysis

Membrane proteins were isolated by carbonate extraction as described in [26]. The details are described in supplementary information. Protein concentration was determined using the 2D Quant kit (GE Healthcare). LC-MS/MS-based spectral counting was performed at the OSU Proteomics Facilities using LTQ-OrbitrapXL mass spectrometer. Proteins were identified using Mascot (v.2.2.2 from Matrix Science, Boston, MA, USA) and a database generated by *in silico* digestion of the *P. aeruginosa* PAO1 proteome predicted from the genome. Search results were validated using Scaffold (v.3 from Proteome Software Inc., Portland, OR). Proteins were considered identified if the protein probability threshold was greater than 99 % and at least three peptides were identified, each with 95 % certainty.

## Expression and reconstitution of aequorin

PAO1 and transposon mutants were transformed with pMMB66EH (courtesy of Dr. Delfina Dominguez), carrying aequorin [27] and carbenicillin resistance genes, using a heat shock method described in [28]. The transformants were selected on Luria bertani (LB) agar containing carbenicillin (300 μg/ml) and, in case of transposon mutants, tetracycline (60 μg /ml) and verified by PCR using aequorin specific primers (For: 5'CTTACATCAGACTTCGACAACCCAAG, Rev: 5'CGTAGAGCTTCTTAGGGCACAG). Aequorin was expressed and reconstituted as described in [9] with modifications. The details are described in supplementary information.

## Luminescence measurements and estimation of free intracellular calcium

Cells with reconstituted aequorin were aliquoted (100 μl) in 96 well plate (Griener bio one, Lumitrack 600) and, when required, treated with inhibitors (2, 4 di-nitrophenol at 0.5, 1, or 2 mM; $LaCl_3$ at 300 or 600 μM; gramicidin D at 1 or 10 μg/ml; calcimycin at 5 μM; or vanadate at 2 mM) for 10 min in the dark at room temperature without shaking. Gramicidin D and calcimycin were dissolved in 50 % and 3 % DMSO, respectively. To ensure

penetration of gramicidin D and calcimycin through the bacterial outer membrane, we added 10 μg/ml of compound 48/80, known to permeabilize the outer membrane of gram negative bacteria without affecting the cytoplasmic membrane [29]. In this case, the corresponding amounts of DMSO and 48/80 were used to treat cells as a negative control. Luminescence was measured at 25 °C using Synergy Mx Multi-Mode Microplate Reader (Biotek). To measure the basal level of $[Ca^{2+}]_{in}$, the measurements were recorded for 1 min at 4 sec interval, then the cells were challenged with 1 or 5 mM $Ca^{2+}$ (final concentration) injected by using the internal Synergy injectors, mixed for 1 sec, and the luminescence was recorded for 20 min at 4-5 sec interval. Injection of buffer alone was used as a negative control, and did not cause any significant fluctuations in $[Ca^{2+}]_{in}$. $[Ca^{2+}]_{in}$ was calculated by using the formula $pCa= 0.612 (-\log_{10}k) + 3.745$, where k is a rate constant for luminescence decay ($s^{-1}$) [9]. The excel-based template incorporating the formula and the aequorin standard curve was generously shared by Dr. Anthony Campbell. The results were normalized against the total amount of available aequorin, which was estimated by summing the light detected during an entire experiment and the light detected during discharge. The discharge was performed by permeabilizing cells with 2 % Nonidet 40 (NP40) in the presence of 12.5 mM $CaCl_2$. The luminescence released during the discharge was monitored for 5 min at 4-5 sec interval. The estimated remaining available aequorin was at least 10 % of the total aequorin, unless mentioned otherwise. To control possible cell lysis and aequorin leakage during the procedure, following the luminescence measurements, the cells were collected by centrifugation, and luminescence was reported for both the supernatants and the cell pellets resuspended in buffer (25 mM HEPES, 1 mM $MgCl_2$, 125 mM NaCl; pH 7.5). The experimental conditions reported here were optimized to prevent any significant cell lysis. The responses to $Ca^{2+}$ challenges were characterized and validated by using curve fitting analysis with IGOR PRO software v.6.3.1.2. (WaveMetrics).

## $Ca^{2+}$ Tolerance Assay

To test cell tolerance to high $Ca^{2+}$, PAO1 and mutants were grown at 5 or 100 mM $Ca^{2+}$. Mid-log cultures grown in 5-ml BMM were inoculated (1 %) into 200 μl of fresh BMM (no added, 5 or 100 mM $Ca^{2+}$) in 96 well plates. The plates were incubated for 12, 24 h or 48 h, and the $OD_{600}$ was measured using Synergy Mx Multi-Mode Microplate Reader (Biotek). The tolerance to $Ca^{2+}$ was calculated as a ratio of $OD_{600}$ of the cultures grown at elevated $Ca^{2+}$ to the cultures grown at no added $Ca^{2+}$. For the wild type PAO1, this ratio equals one.

## Swarming Assay

Swarming motility was assayed as described in [30]. PAO1 and mutants were grown in BMM at 0 mM or 5 mM $Ca^{2+}$. 2 μl of the mid log cultures normalized to the OD600 of 0.3 were spot inoculated onto the surface of swarming agar [30]. When needed, inhibitors (10 μg/ml gramicidin D, 2 mM vanadate, or 600 μM $LaCl_3$) were added. Gramicidin D was dissolved in DMSO and added with compound 48/80 (10 μg/ ml). After inoculation, the plates were incubated for 16 h and the colony diameters were measured. The effect of $Ca^{2+}$ was calculated as a fold difference (ratio) between the diameters of the colonies grown at 5 mM and 0 mM $Ca^{2+}$. The mutants and treatments were compared to their corresponding controls using the mean percentage of fold difference from at least three independent experiments.

## RESULTS

### *P. aeruginosa* maintains $[Ca^{2+}]_{in}$ homeostasis

To study $Ca^{2+}$ homeostasis in *P. aeruginosa* PAO1, we first measured the basal level of free intracellular $Ca^{2+}$ ($[Ca^{2+}]_{in}$), and then monitored the changes in $[Ca^{2+}]_{in}$ in response to externally added 1 and 5 mM $Ca^{2+}$. Cells grown at no added $Ca^{2+}$ (naïve) or 5 mM $Ca^{2+}$ (induced) were compared. In naïve cells, the $[Ca^{2+}]_{in}$ was 0.14 ± 0.05 μM (Fig. 1A). The addition of 1 mM $Ca^{2+}$ caused a 13 fold increase of $[Ca^{2+}]_{in}$ to 1.86 ± 0.53 μM within 0.6 min (2.92 μM/min) followed by a two-phase decline, validated by the curve fitting analysis. The first, fast, phase proceeded at a rate 0.75 μM/min, lasted for ~2 min, and accounted for 38 % of $[Ca^{2+}]_{in}$ reduction. During the second, slow, phase, $[Ca^{2+}]_{in}$ reduced for another 35% to 0.5 μM at a rate 0.04 μM/min. When the cells were transferred to a fresh buffer containing no $Ca^{2+}$, a complete recovery to the basal $[Ca^{2+}]_{in}$ level was observed (data not shown). We also monitored $[Ca^{2+}]_{in}$ for additional 70 min and detected a very slow decrease at a rate 1.43 nM/min (data not shown). Considering the minor changes during this extended incubation, $[Ca^{2+}]_{in}$ was monitored during 21 min in all further experiments. Challenging naïve cells with 5 mM $Ca^{2+}$ caused 28 fold increase in $[Ca^{2+}]_{in}$ to 3.93 ± 0.37 μM within 0.92 min (3.88 μM/min) followed by a multi-phase decrease. First, $[Ca^{2+}]_{in}$ dropped similarly to naïve cells by 38 %, but at a lower rate 0.46 μM/min. Then it increased to 3.01 ± 0.34 μM and slowly declined to 2.22 μM, showing a total decrease by 44 %.

In induced cells, the basal $[Ca^{2+}]_{in}$ was 0.22 ± 0.04 μM, which is 57 % higher than in naïve cells (Fig. 1B). Upon exposure to 1 mM $Ca^{2+}$, the induced cells increased their $[Ca^{2+}]_{in}$ at a rate (3.12 μM/min) similar to naïve cells, but only fivefold (to 1.19 ± 0.11 μM) and during a shorter period of time (0.3 min). The following decrease proceeded with a much lower rate (0.16 μM/min), lasted for ~1.5 min, and accounted for 21 %. In contrast to naïve cells, during the second phase, $[Ca^{2+}]_{in}$ slowly increased with a rate 0.04 μM/min to 1.23 ± 0.45 μM. The response to 5 mM $Ca^{2+}$ in induced cells also showed a multi-phase pattern. Although the first rapid increase brought $[Ca^{2+}]_{in}$ to a similar to naïve cells level (3.66 ± 0.44 μM), it was only 17 fold higher than the basal level. This increase occurred very quickly within 0.08 min at a rate 42.62 μM/min. The following decline was threefold faster than in naïve cells (1.6 μM/min). The second increase was similar to the one in naïve cells elevating $[Ca^{2+}]_{in}$ to 2.9 ± 0.45 μM, followed by a decline to 2.13 ± 0.27 μM with a total decrease by 42 %.

### The PAO1 genome contains multiple homologs of $Ca^{2+}$ transporting ATPases and gradient driven exchangers

Homology searches in the PAO1 genome (www.pseudomonas.com) using amino acid sequences of the characterized prokaryotic $Ca^{2+}$ transporters revealed 18 genes encoding different types of transporters (Table 1). Based on sequence similarity and predicted conserved domains, ten were predicted to encode P-, F-type, and ABC-type ATPases, and eight to encode ion exchangers and other types of transporters. They include two earlier characterized proteins: heavy metal translocating P-type ATPase (PA2435) and dicarboxylic acid transporter (PA5167) [31, 32]. The comparative sequence analyses revealed that seven predicted P-type ATPases share 13 - 39 % sequence identity and do not have other paralogs

in the PAO1 genome. Phylogenetic analysis using functionally characterized prokaryotic P-type ATPases showed that the PAO1 proteins can be grouped into four clades, which coincide with ion specificity: 1) $Ca^{2+}$ (PA1429); 2) $Mg^{2+}$ (PA4825); 3) $K^{+}$ (PA1634); and 4) $Pb^{2+}$, $Cd^{2+}$, $Zn^{2+}$, $CO^{2+}$, $Cu^{2+}$ (PA2435, PA3920, PA1549, and PA3690) (Fig. S1). Further sequence comparison revealed that PA1429 together with five prokaryotic $Ca^{2+}$-translocating P-type ATPases in clade 1 are more closely related to the human $Ca^{2+}$ translocating ATPase SERCA than to the human calmodulin-binding ATPase PMCA1 (data not shown). This supports their classification into the subgroup of P2A-ATPases [20]. Interestingly, clade 2, including PA4825 and $Mg^{2+}$-translocating MgtB from *S. typhimurium*, is closely related to PMCA1 (data not shown). Furthermore, considering that PA2435 was shown to uptake both $Cu^{2+}$ and $Zn^{2+}$ [32], we combined $Cu^{2+}$ and heavy metal- translocating proteins into one clade (4). As a result, PA1549, earlier grouped into functionally uncharacterized subfamily FUPA27 [33], was clustered with clade 4 proteins, suggesting its possible involvement in translocation of these ions. Other predicted transporters have one to four paralogs in the PAO1 genome and share 28 % – 82 % amino acid sequence identity. All the predicted transporters are conserved among ten sequenced pseudomonads and share 19 % – 100 % identity with their corresponding homologs.

## Growth at elevated $Ca^{2+}$ alters abundance of PAO1 membrane proteins

The modulated $[Ca^{2+}]_{in}$ response in $Ca^{2+}$ induced cells suggested the involvement of transporters, whose expression is affected by $Ca^{2+}$. To identify such transporters, membrane proteins from PAO1 cells grown at no added or 5 mM $Ca^{2+}$ were extracted and subjected to LC-MS/MS spectral counting - based comparative analyses. In total, about 500 proteins were identified, of which more than 80 % were transmembrane or membrane-associated proteins. These included seven bioinformatically predicted putative $Ca^{2+}$ transporters, and ten proteins encoded within the same apparent operons (Table 1). To estimate the effect of $Ca^{2+}$, for every protein we calculated a ratio of the total number of fragmentation spectra that map to the peptides of the protein in the samples collected at 5 mM *vs*. no added $Ca^{2+}$. The results suggest that six predicted $Ca^{2+}$ transporters (shown in bold in Table 1) increased abundance at least twofold in response to growth at elevated $Ca^{2+}$. Considering that apparent operonic genes may have similar expression profile, the results also suggest $Ca^{2+}$ induction for PA3400, PA5167, PA4016, and PA1549. However, PA4496 and PA4497 showed decreased abundance in response to 5 mM $Ca^{2+}$.

## $Ca^{2+}$ homeostasis in PAO1 involves multiple transporters of different types

To study the role of the predicted transporters in $Ca^{2+}$ homeostasis, we obtained 18 mutants, each with one predicted transporter encoding gene disrupted with either ISphoA/hah or ISlacZ/hah transposon insertion. The mutants were monitored for their $[Ca^{2+}]_{in}$ response to 1 mM $Ca^{2+}$ and compared to the wild type (WT) PAO1 cells. Based on the results they were grouped into four groups (Fig 2). Group I (four mutants) showed the initial rapid increase in $[Ca^{2+}]_{in}$ at least twofold higher than in WT cells followed by the recovery to approximately the WT level $[Ca^{2+}]_{in}$. Group II (five mutants) failed the recovery to the WT level $[Ca^{2+}]_{in}$ during 21 min monitoring, and had the remaining $[Ca^{2+}]_{in}$ at the levels at least twofold higher than in PAO1 cells. Group III (four mutants) showed two peaks of $[Ca^{2+}]_{in}$ increase and the remaining $[Ca^{2+}]_{in}$ at the level at least twofold higher than in WT cells. The $[Ca^{2+}]_{in}$

changes less than twofold *vs*. PAO1 were considered not significant (five mutants in group IV).

Among the ten examined mutants with disrupted putative ATP-ases, seven showed significant changes in $[Ca^{2+}]_{in}$ response (Fig 2A). They included mutants lacking six P-type ATPases: PA3690, PA4825 (Group I), PA1429, PA1549 (Group II), PA2435, PA3920 (Group III), and ABC transporter PA3400 (Group II). The group III mutants showed the most drastic changes in $[Ca^{2+}]_{in}$ response, and together with PA1549-lacking mutant failed to significantly decrease the elevated $[Ca^{2+}]_{in}$. The remaining three ATP-ases: P-type PA1634, F-type PA5554, and ABC transporter PA4496 showed no role in maintaining $[Ca^{2+}]_{in}$ homeostasis (Group IV). Among the eight tested putative ion exchangers and other transporters, disruption of six showed significant changes in $[Ca^{2+}]_{in}$ response (Fig. 2B). They included: three ion exchangers PA3963, PA4292 (Group I), and PA2092 (Group III), dicarboxylic acid transporter PA5167, hypothetical protein PA4016 (Group II), and mechanosensitive channel PA4614 (Group III). Among these proteins, the most significant effect was observed for the mutant lacking a major facilitator type transporter PA2092, that was unable to reduce $[Ca^{2+}]_{in}$ after the initial increase. Ion exchanger PA0397 and probable $Na^+$ translocating oxidoreductase PA2999 showed no role in $Ca^{2+}$ homeostasis.

## Multiple mechanisms are involved in Ca $^{2+}$ homeostasis in PAO1

To identify the role of different types of transporters in $Ca^{2+}$ homeostasis and better understand the mutants $[Ca^{2+}]_{in}$ profiles, we examined the effect of several inhibitors specifically affecting different mechanisms associated with ion transport, on the maintenance of $[Ca^{2+}]_{in}$. For this, PAO1 cells were treated with the selected inhibitors and monitored for their $[Ca^{2+}]_{in}$ response to 1 mM $Ca^{2+}$. First, calcimycin, a $Ca^{2+}$ ionophore known to carry $Ca^{2+}$ into the cells [34], was used to test the response of PAO1 cells to $Ca^{2+}$ influx (Fig. 3A). Treatment with 5 μM calcimycin caused a rapid (36 μM/min) uptake of $Ca^{2+}$ and increase of $[Ca^{2+}]_{in}$ to 9.54 ± 0.15 μM followed by an immediate but slower (4.1 μM/min) decline to 2.36 ± 0.33 μM. The second increase in $[Ca^{2+}]_{in}$ , although appearing 4 min earlier than in the DMSO control, is most likely due to the presence of DMSO (used to dissolve calcimycin).

To test the role of a proton gradient across the cytoplasmic membrane and intracellular ATP in $[Ca^{2+}]_{in}$ response, 2,4-Dinitrophenol (DNP), a proton ionophore known to disrupt a proton gradient and uncouple oxidative phosphorylation [25], was used (Fig. 3B). In a concentration dependent manner, DNP caused a second peak of $[Ca^{2+}]_{in}$ to increase, which at higher levels of DNP appeared to merge with the first peak and reached 7.28 ± 0.74 μM. This level of $[Ca^{2+}]_{in}$ was reached at the rate of 22 fold slower than in calcimycin-treated cells, and was followed by a 32 % decrease. The remaining $[Ca^{2+}]_{in}$ was higher with increasing dose of DNP, and at 2 mM DNP, reached 8.39 ± 1.35 μM.

To examine the role of monovalent cation exchangers in PAO1 $Ca^{2+}$ homeostasis, gramicidin D treatment was used (Fig. 3C). Gramicidin D is known to form channels across the cytoplasmic membrane and dissipate the gradients of $H^+$, $Na^+$, and $K^+$ [35], which may also affect the intracellular ATP pool [36]. In a concentration-dependent manner, gramicidin D treatment elevated the initial increase in $[Ca^{2+}]_{in}$ up to 9.06 ± 1.15 μM, which was

followed by a decline to 2.49 ± 0.23 μM. The rates of $[Ca^{2+}]_{in}$ increase and decrease were at least twofold higher at 10 μg/ml than at 1 μg/ml gramicidin D. The $[Ca^{2+}]_{in}$ recovery levels were similar in the treated cells and at least fivefold higher than in the untreated cells. The effect of gramicidin D on $[Ca^{2+}]_{in}$ also included the effect caused by DMSO.

Lanthanum (III) is a $Ca^{2+}$ antagonist, known to block $Ca^{2+}$ channels [37]. It may also arrest $Ca^{2+}$-binding ATPases in a phosphorylated form and prevent further conformational changes required for $Ca^{2+}$ translocation [38]. The effect of $LaCl_3$ on the level of $[Ca^{2+}]_{in}$ showed two distinct concentration-dependent patterns: a decrease in the initial rise in $[Ca^{2+}]_{in}$ and appearance of the second peak of $[Ca^{2+}]_{in}$ (Fig. 3D). The remaining level of $Ca^{2+}{}_{in}$ was at least fivefold higher in the $LaCl_3$ treated cells than in the untreated.

We also tested the effect of vanadate on $Ca^{2+}$ homeostasis in PAO1 (Fig. 3E). Vanadate is known to inhibit P-type [39] and ABC [40] ATPases, and therefore is expected to block $Ca^{2+}$ uptake or efflux mediated by these transporters. Vanadate treatment increased the initial rise of $[Ca^{2+}]_{in}$ by twofold, and the remaining level of $[Ca^{2+}]_{in}$ by fourfold.

### $Ca^{2+}$ homeostasis is not involved in PAO1 tolerance to external $Ca^{2+}$

To examine whether the putative $Ca^{2+}$ transporters play a role in cell tolerance to high $Ca^{2+}$, thirteen mutants from groups I - III were grown in the presence of 5 or 100 mM $Ca^{2+}$ and compared to WT. The results showed that at 5 mM $Ca^{2+}$, neither PAO1 nor mutants showed any growth defects. Similarly, the addition of 100 mM $Ca^{2+}$, although introduced a 13 h lag phase, did not significantly affect growth of the wild type or the mutants (data not shown).

### $Ca^{2+}$ homeostasis is involved in regulating $Ca^{2+}$-induced swarming motility in PAO1

To determine the role of $Ca^{2+}$ homeostasis in $Ca^{2+}$- induced swarming motility in PAO1, the group III mutants with abolished ability to maintain $Ca^{2+}$ homeostasis were tested for swarming motility at 5 mM $Ca^{2+}$ *vs*. no added $Ca^{2+}$ (Fig. 4 A). The presence of $Ca^{2+}$ induced swarming in PAO1 by sixfold. When this induction was taken as 100 %, two mutants PA3920:IS, with disrupted P-type ATPase, and PA2092:IS, with disrupted major facilitator protein, showed only 27 % and 67 % of $Ca^{2+}$ induction, respectively. PA2435:IS, with disrupted P-type ATPase, showed no significant difference in swarming, and PA4614:IS, with disrupted mechanosensitive channel, swarmed 26 % further in the presence of $Ca^{2+}$ than PAO1. We also tested the effect of inhibitors targeting P-type and ABC ATPases (vanadate), $Ca^{2+}$ channels ($LaCl_3$), or dissipating $H^+$, $Na^+$, and $K^+$ gradients (gramicidin D) on $Ca^{2+}$-induced swarming motility (Fig. 4 B). All three inhibitors reduced the effect of $Ca^{2+}$ on swarming. The most significant reduction was observed in the presence of 2 mM vanadate, where $Ca^{2+}$ induction reached only 17 % of the induction in untreated PAO1. The presence of 10 μg/ml gramicidin D or 600 μM $LaCl_3$ decreased $Ca^{2+}$ induction by 34% and 63%, respectively. The results for $LaCl_3$ should, however, be taken with a caution, since it precipitated during preparation.

## DISCUSSION

This study establishes that *Pseudomonas aeruginosa* PAO1, a human pathogen with $Ca^{2+}$-induced virulence, maintains free intracellular $Ca^{2+}$ at sub-micromolar level, which rapidly

increases and slowly restores in response to external $Ca^{2+}$. This process is impaired by blocking monovalent cation gradient or modulating $Ca^{2+}$ uptake, and requires several transporters from the superfamilies of P-type ATPases and ion exchangers. These proteins will make an excellent tool for studying $Ca^{2+}$ regulation and signaling in this organism. Finally, the study showed the role of $Ca^{2+}$ homeostasis in $Ca^{2+}$- induced swarming motility, suggesting its regulatory role in *P. aeruginosa* response to $Ca^{2+}$.

The intracellular level of $[Ca^{2+}]_{in}$ (0.1 – 0.2 μM) and the magnitude (5-28 fold) of the initial response to external $Ca^{2+}$ (1 - 5 mM) places *P. aeruginosa* among three other bacteria *E. coli* JM109, *Anabaena sp*. PCC7120, and *B. subtilis* [9, 12, 13], whose intracellular $Ca^{2+}$ levels have been characterized. In contrast, *Propionibacterium acne*, although has a similar basal level of $[Ca^{2+}]_{in}$, responds to 1mM $Ca^{2+}$ by only twofold increase in $[Ca^{2+}]_{in}$ [10]. The results illustrate that *P. aeruginosa* is able to maintain sub-micromolar levels of intracellular $Ca^{2+}$ in the presence of millimolar levels of external $Ca^{2+}$, suggesting its ability to (1) block $Ca^{2+}$ uptake, (2) pump out $Ca^{2+}$ from the cells against the steep concentration gradient, or (3) chelate $Ca^{2+}$ inside the cells. The first two abilities in prokaryotes were attributed to the function of several mechanisms including ion channels, P- and F-type ATPases and ion gradient driven transporters that were identified using inhibitors [13, 25] or individual proteins [22].

The detected two-phase $[Ca^{2+}]_{in}$ recovery (short-rapid and long-slow) following the challenge with 1 mM $Ca^{2+}$ may suggest the function of distinct efflux mechanisms of high and low efficiency. The following fluctuations of $[Ca^{2+}]_{in}$ in the presence of 5 mM $Ca^{2+}$ may be a result of continuous cumulative effect of both influx and efflux mechanisms eventually resulting in the recovery of the $[Ca^{2+}]_{in}$ basal level. Comparison of $Ca^{2+}$-induced and naïve cells revealed multiple differences in $[Ca^{2+}]_{in}$ responses. Lower initial $[Ca^{2+}]_{in}$ responses with elevated rates of the $[Ca^{2+}]_{in}$ initial increase and decrease in the presence of 5 mM $Ca^{2+}$ in induced cells suggest that $Ca^{2+}$ induces adaptation mechanisms. However, the elevated basal level of $[Ca^{2+}]_{in}$ in induced cells and their inability to significantly reduce the increased $[Ca^{2+}]_{in}$ at 1 mM $Ca^{2+}$ indicate that growth at elevated $Ca^{2+}$ possibly sensitizes cells to external $Ca^{2+}$, as was proposed in *E. coli* [9]. Overall, these observations suggest the presence of multiple mechanisms for controlling $Ca^{2+}$ homeostasis in *P. aeruginosa* and their complex regulation in response to different levels of $Ca^{2+}$ in the environment.

Among several types of transporters determined to be involved in the maintenance of $[Ca^{2+}]_{in}$ homeostasis, the most numerous were P-type ATPases. This superfamily of transporters has long been established to transport metals, but was not initially considered to play a major role in $Ca^{2+}$ transport in prokaryotes. Later, several reports described both $Ca^{2+}$-dependent P-type ATPase activity and ATP-dependent $Ca^{2+}$ transport or transporters, most of which were shown to efflux $Ca^{2+}$ *in-vitro* in membrane vesicles [21, 41]. However their role in maintaining cellular $Ca^{2+}$ homeostasis *in-vivo* has not been tested. In this study, out of the seven P-type ATPases predicted in the PAO1 genome, four were induced by $Ca^{2+}$, and six played a role in $[Ca^{2+}]_{in}$ maintenance. These six were phylogenetically related to divalent cation translocating ATPases, whereas PA1634 clustered with $K^+$-translocating KdpB from *E. coli*, showed no effect on $[Ca^{2+}]_{in}$ homeostasis. P-type ATPases are known to be inhibited by vanadate, functioning as a phosphate analog [39]. In agreement, four mutants

with disrupted P-type ATPases showed a $[Ca^{2+}]_{in}$ profile similar to the profile of vanadate treated PAO1 cells with increased $[Ca^{2+}]_{in}$ or lowered ability of its recovery. The disruption of two other P-type ATPases PA2435 and PA3920 showed the most significant effect and abolished the ability of PAO1 to reduce $[Ca^{2+}]_{in}$ below 1.5 μM in the presence of 1mM $Ca^{2+}$. PA2435 has been shown earlier to translocate $Cu^{2+}$and $Zn^{2+}$ [32], but in our phylogenetic analysis, it clustered closer to heavy metal-translocating ATPases, whereas PA3920 was more closely related to $Cu^{2+}$-translocating transporters. Noteworthy, these two proteins were not detected to be induced by $Ca^{2+}$, and therefore, likely do not contribute to the increased rate of $Ca^{2+}$ efflux in $Ca^{2+}$-induced cells. Since the identified P-type ATPases contributing to the detected changes in the intracellular $Ca^{2+}$ do not contain typical $Ca^{2+}$-binding domains, they are not likely to play a direct role in translocating $Ca^{2+}$. The ATPases may be involved in controlling transition of metals important for $Ca^{2+}$ translocation or generating an ion gradient that serves as an energy source for $Ca^{2+}$ transporters, as was proposed in *A. vinelandii* [42].

To characterize the contribution of F-type ATPases (ATP synthases) in $Ca^{2+}$ homeostasis, we treated cells with a protonophore 2,4 DNP, known to inhibit ATP synthesis by uncoupling oxidative phosphorylation [25]. This treatment raised the level of $[Ca^{2+}]_{in}$ and impaired the ability of PAO1 to decrease it, most likely due to the lack of ATP. The role of ATP in $Ca^{2+}$ efflux has been described in *E. coli*, where the lack of F-type ATP synthase AtpD decreased cellular ATP content and impaired $[Ca^{2+}]_{in}$ efflux [25]. However, the disruption of PA5554, the AtpD homolog with 82 % amino acid sequence identity, although induced by $Ca^{2+}$, did not affect $Ca^{2+}$ homeostasis. It is possible that two paralogs of PA5554 in the genome: PA1697 and PA1104, with 24 and 28 % amino acid sequence identity, correspondingly, could compensate for the absence of PA5554 and provide ATP required for $Ca^{2+}$ efflux.

Gradient driven $Ca^{2+}$ exchangers have been considered as a major mechanism in bacterial $Ca^{2+}$ efflux that most commonly employs $H^+$ and $Na^+$ as coupling ions. In agreement, treating PAO1 with gramicidin D, known to dissipate monovalent ion gradients across the cytoplasmic membrane [34], caused a significant initial accumulation of $[Ca^{2+}]_{in}$, which decreased over time, suggesting the function of alternative efflux mechanisms. We predicted and tested the role of four putative gradient driven exchangers in $[Ca^{2+}]_{in}$ homeostasis, three of which showed a significant impact on $Ca^{2+}$ homeostasis. The disruption of PA2092 showed the most prominent effect, as the mutant was not able to decrease the elevated $[Ca^{2+}]_{in}$ in the presence of 1mM $Ca^{2+}$. None of the predicted ion exchangers were induced by $Ca^{2+}$, suggesting that, similarly to P-type ATPases PA2435 and PA3920, they do not play role in the differences between naïve and induced cells. The results suggest that $Ca^{2+}$ translocation may be coordinated by the combined action of both P-type ATPases and ion exchangers as was illustrated for SERCA or PMCA ATPases and $Na^+/Ca^{2+}$ exchangers in mammalian systems [43, 44].

Treating PAO1 cells with a $Ca^{2+}$ channel blocker $LaCl_3$ [37] reduced the initial uptake of $Ca^{2+}$, confirming the role of $La^{3+}$ sensitive channels in PAO1 $Ca^{2+}$ influx, as has been shown in other bacteria [9, 13]. The antagonistic effect of $La^{3+}$ on $Ca^{2+}$ influx in *E. coli* was associated with poly-3-hydroxybutyrate/polyphosphate (PHB-PP) channels [9]. However,

search of the PAO1 genome for homologs of the functionally defined PHB-PP genes from *Ralstonia* [45] returned only scattered homologous genes. This may indicate the presence of a non- or low-homology PHB-PP biosynthetic pathway or a different type of $La^{3+}$ sensitive channels in PAO1. Interestingly, in addition to blocking $Ca^{2+}$ influx, $LaCl_3$ treatment caused a secondary $[Ca^{2+}]_{in}$ increase and a plateau at about 3 μM. This suggests that $La^{3+}$ also inhibits $Ca^{2+}$ efflux, which is consistent with the known inhibition effect of $La^{3+}$ on P-type ATPases *via* blocking phosphorylation events [20, 38]. Furthermore, we detected that the disruption of PA4614 encoding $Ca^{2+}$-induced probable mechanosensitive channel MscL caused a very quick uptake of $Ca^{2+}$ followed by a second increase and a slow recovery of $[Ca^{2+}]_{in}$. In *E. coli*, although the expression of the homologous gene was also affected by $Ca^{2+}$, its disruption showed no effect on $Ca^{2+}$ homeostasis [25]. Mechanosensitive channels are known to open in response to membrane tension and protect cells against hypoosmotic shock as reviewed in [46]. It is not clear why the lack of the MscL protein caused the increase in $Ca^{2+}$ uptake. We hypothesize that $Ca^{2+}$-induced MscL may contribute to limiting $Ca^{2+}$ uptake when in a closed state under the tested physiological conditions, and when *mscL* is disrupted, cells become more permeable to $Ca^{2+}$ influx.

Finally, we determined that elevated $Ca^{2+}$ induced swarming motility in PAO1, whereas treatment with vanadate, $LaCl_3$ and gramicidin D decreased this induction. The disruption of P-type ATPase PA3920 and ion exchanger PA2092 also significantly diminished the inducing effect of $Ca^{2+}$ on swarming. The effect of $Ca^{2+}$ on swarming motility varies in different bacteria, for example, $Ca^{2+}$ has been shown to induce swarming in *Vibrio parahaemolyticus* [47], but inhibited this type of motility in fluorescent pseudomonads [48]. This study shows for the first time that $Ca^{2+}$ homeostasis plays an important role in *P. aeruginosa* $Ca^{2+}$ induced swarming, a complex physiological phenomenon known to modulate virulence and antibiotic resistance in this organism [49].

Overall, this study reports that *P. aeruginosa* PAO1 maintains a sub-micromolar basal level of $[Ca^{2+}]_{in}$ using multiple transport mechanisms that most likely require ATP and monovalent cation gradient. Involvement of multiple transport systems in $Ca^{2+}$ influx and efflux has been suggested in *E. coli* [9, 50], and may be differentially regulated by growth conditions. This functional redundancy was also illustrated by the high tolerance of PAO1 cells to external $Ca^{2+}$, and reflects the physiological importance of the controlled cellular $Ca^{2+}$ homeostasis. The two major aspects of such importance include protecting cells against the toxicity of high $[Ca^{2+}]$ and maintaining low basal level of $[Ca^{2+}]_{in}$ required for $Ca^{2+}$ to play a signaling role. The transient changes in $[Ca^{2+}]_{in}$ (magnitude, length, and frequency) may function to relate external signal(s) to cellular response(s), as has been established in eukaryotes [1] and proposed in prokaryotes [5]. We identified at least three transporters that play a major role in $[Ca^{2+}]_{in}$ homeostasis, and will be used in further studies required for experimental confirmation of signaling role of $Ca^{2+}$ in *P. aeruginosa*.

## Supplementary Material

Refer to Web version on PubMed Central for supplementary material.

## ACKNOWLEDGEMENTS

We thank Dr. Anthony Campbell from the School of Pharmacy and Pharmaceutical Sciences, Cardiff University in UK for sharing his expertise and the templates for calculating $[Ca^{2+}]_{in}$. We thank Dr. Delfina Dominguez from The University of Texas at El Paso for sharing *E. coli* strain carrying pMMB66EH. We thank Dr. Wouter Hoff from Oklahoma State University for critical review of the manuscript and insightful discussions. We thank Dr. Masato Kumauchi from Oklahoma State University for curve-fitting analysis. Mass spectrometry analyses were performed in the DNA/Protein Resource Facility at Oklahoma State University, using resources supported by the NSF MRI and EPSCoR programs (Award DBI/0722494). This work was supported by the Grant-in-Aid from American Heart Association (Award 09BGIA2330036) and the Research Grant from OCAST (Award HR12-167). Transposon mutants were obtained from the University of Washington Two - Allele library (grant # NIH P30 DK 089507).

## REFERENCES

1. Clapham DE. Calcium signaling. Cell. 2007; 131:1047–1058. [PubMed: 18083096]
2. Liu L, Ridefelt P, Hakansson L, Venge P. Regulation of human eosinophil migration across lung epithelial monolayers by distinct calcium signaling mechanisms in the two cell types. Journal of immunology (Baltimore, Md. 1999; 163:5649–5655.
3. Halmerbauer G, Arri S, Schierl M, Strauch E, Koller DY. The relationship of eosinophil granule proteins to ions in the sputum of patients with cystic fibrosis. Clin Exp Allergy. 2000; 30:1771–1776. [PubMed: 11122216]
4. Lorin MI, Gaerlan PF, Mandel ID, Denning CR. Composition of nasal secretion in patients with cystic fibrosis. The Journal of laboratory and clinical medicine. 1976; 88:114–117. [PubMed: 932530]
5. Dominguez DC. Calcium signalling in bacteria. Molecular microbiology. 2004; 54:291–297. [PubMed: 15469503]
6. Sarkisova S, Patrauchan MA, Berglund D, Nivens DE, Franklin MJ. Calcium-induced virulence factors associated with the extracellular matrix of mucoid *Pseudomonas aeruginosa* biofilms. Journal of bacteriology. 2005; 187:4327–4337. [PubMed: 15968041]
7. Patrauchan MA, Sarkisova SA, Franklin MJ. Strain-specific proteome responses of *Pseudomonas aeruginosa* to biofilm-associated growth and to calcium. Microbiology+. 2007; 153:3838–3851. [PubMed: 17975093]
8. Domníguez DC LR, Holland IB, Campbell AK. Proteome analysis of *B. subtilis* in response to calcium. J Anal Bioanal Techniques. 2011; S6
9. Jones HE, Holland IB, Baker HL, Campbell AK. Slow changes in cytosolic free $Ca^{2+}$ in *Escherichia coli* highlight two putative influx mechanisms in response to changes in extracellular calcium. Cell calcium. 1999; 25:265–274. [PubMed: 10378087]
10. Futsaether CM, Johnsson A. Using fura-2 to measure intracellular free calcium in *Propionibacterium acnes*. Canadian journal of microbiology. 1994; 40:439–445. [PubMed: 8050064]
11. Rosch JW, Sublett J, Gao G, Wang YD, Tuomanen EI. Calcium efflux is essential for bacterial survival in the eukaryotic host. Molecular microbiology. 2008; 70:435–444. [PubMed: 18761687]
12. Herbaud ML, Guiseppi A, Denizot F, Haiech J, Kilhoffer MC. Calcium signalling in *Bacillus subtilis*. Bba-Mol Cell Res. 1998; 1448:212–226.
13. Torrecilla I, Leganes F, Bonilla I, Fernandez-Pinas F. Use of recombinant aequorin to study calcium homeostasis and monitor calcium transients in response to heat and cold shock in cyanobacterial. Plant Physiol. 2000; 123:161–175. [PubMed: 10806234]
14. Leganes F, Forchhammer K, Fernandez-Pinas F. Role of calcium in acclimation of the cyanobacterium *Synechococcus elongatus* PCC 7942 to nitrogen starvation. Microbiol-Sgm. 2009; 155:25–34.
15. Campbell AK, Naseern R, Holland IB, Matthews SB, Wann KT. Methylglyoxal and other carbohydrate metabolites induce lanthanum-sensitive $Ca^{2+}$ transients and inhibit growth in *E.coli*. Arch Biochem Biophys. 2007; 468:107–113. [PubMed: 17961498]

16. Rosen BP. Bacterial calcium transport. Biochimica et biophysica acta. 1987; 906:101–110. [PubMed: 2436666]
17. Fujisawa M, Wada Y, Tsuchiya T, Ito M. Characterization of *Bacillus subtilis* YfkE (ChaA): a calcium-specific $Ca^{2+}/H^{+}$ antiporter of the CaCA family. Arch Microbiol. 2009; 191:649–657. [PubMed: 19543710]
18. Waditee R, Hossain GS, Tanaka Y, Nakamura T, Shikata M, Takano J, Takabe T, Takabe T. Isolation and functional characterization of $Ca^{2+}/H^{+}$ antiporters from cyanobacteria. Journal of Biological Chemistry. 2004; 279:4330–4338. [PubMed: 14559898]
19. Radchenko MV, Tanaka K, Waditee R, Oshimi S, Matsuzaki Y, Fukuhara M, Kobayashi H, Takabe T, Nakamura T. Potassium/proton antiport system of *Escherichia coli*. Journal of Biological Chemistry. 2006; 281:19822–19829. [PubMed: 16687400]
20. Palmgren MG, Nissen P. P-type ATPases. Annual review of biophysics. 2011; 40:243–266.
21. Berkelman T, Garretengele P, Hoffman NE. The Pacl gene of *Synechococcus* Sp strain Pcc-7942 encodes a $Ca^{2+}$-transporting Atpase. Journal of bacteriology. 1994; 176:4430–4436. [PubMed: 8021228]
22. Faxen K, Andersen JL, Gourdon P, Fedosova N, Morth JP, Nissen P, Moller JV. Characterization of a *Listeria monocytogenes* Ca2+ pump a SERCA-type ATPase with only one $Ca^{2+}$-binding site. Journal of Biological Chemistry. 2011; 286:1609–1617. [PubMed: 21047776]
23. Raeymaekers L, Wuytack EY, Willems I, Michiels CW, Wuytack F. Expression of a P-type $Ca^{2+}$-transport ATPase in *Bacillus subtilis* during sporulation. Cell calcium. 2002; 32:93–103. [PubMed: 12161109]
24. Desrosiers MG, Gately LJ, Gambel AM, Menick DR. Purification and characterization of the $Ca^{2+}$-ATPase of *Flavobacterium odoratum*. The Journal of biological chemistry. 1996; 271:3945–3951. [PubMed: 8632017]
25. Naseem R, Wann KT, Holland IB, Campbell AK. ATP regulates calcium efflux and growth in *E. coli*. J Mol Biol. 2009; 391:42–56. [PubMed: 19481094]
26. Nouwens AS, Cordwell SJ, Larsen MR, Molloy MP, Gillings M, Willcox MD, Walsh BJ. Complementing genomics with proteomics: the membrane subproteome of Pseudomonas aeruginosa PAO1. Electrophoresis. 2000; 21:3797–3809. [PubMed: 11271498]
27. Campbell AK, S-NG. Bioluminescent and chemiluminescent indicators for molecular signalling and function in living cells. In: WT, M., editor. Flourescent and Luminescent probes for biological activity. Academic Press; New York: 1993. p. 58-82.
28. Irani VR, Rowe JJ. Enhancement of transformation in *Pseudomonas aeruginosa* PAO1 by $Mg^{2+}$ and heat. BioTechniques. 1997; 22:54–56. [PubMed: 8994645]
29. Katsu T, Kobayashi H, Fujita Y. Mode of Action of Gramicidin S on *Escherichia coli* Membrane. Biochimica et biophysica acta. 1986; 860:608–619. [PubMed: 2427118]
30. Overhage J, Lewenza S, Marr AK, Hancock REW. Identification of genes involved in swarming motility using a *Pseudomonas aeruginosa* PAO1 mini-Tn5-lux mutant library. Journal of bacteriology. 2007; 189:2164–2169. [PubMed: 17158671]
31. Valentini M, Storelli N, Lapouge K. Identification of C(4)-dicarboxylate transport systems in *Pseudomonas aeruginosa* PAO1. Journal of bacteriology. 2011; 193:4307–4316. [PubMed: 21725012]
32. Lewinson O, Lee AT, Rees DC. A P-type ATPase importer that discriminates between essential and toxic transition metals. P Natl Acad Sci USA. 2009; 106:4677–4682.
33. Chan H, Babayan V, Blyumin E, Gandhi C, Hak K, Harake D, Kumar K, Lee P, Li TT, Liu HY, Lo TC, Meyer CJ, Stanford S, Zamora KS, Saier MH Jr. The p-type ATPase superfamily. Journal of molecular microbiology and biotechnology. 2010; 19:5–104. [PubMed: 20962537]
34. Pressman BC. Biological application of ionophores. Annual Review of Biochemistry. 1976; 45:501–530.
35. Burkhart BM, Langs DA, Pangborn WA, Duax WL, Pletnev V, Gassman RM. Gramicidin D conformation, dynamics and membrane ion transport. Biopolymers. 1999; 51:129–144. [PubMed: 10397797]
36. Jarrell KF, Hamilton EA. Effect of gramicidin on methanogenesis by various methanogenic bacteria. Applied and environmental microbiology. 1985; 50:179–182. [PubMed: 16346835]

37. Reusch RN, Huang RP, Bramble LL. Poly-3-hydroxybutyrate polyphosphate complexes from voltage activated Ca2+ channels in the plasma membranes of *Escherichia coli*. Biophys J. 1995; 69:754–766. [PubMed: 8519976]
38. Luterbacher S, Schatzmann HJ. The site of action of $La^{3+}$ in the reaction cycle of the human red cell membrane $Ca^{2+}$-pump ATPase. Experientia. 1983; 39:311–312. [PubMed: 6130967]
39. Kuhlbrandt W. Biology, structure and mechanism of P-type ATPases. Nat Rev Mol Cell Bio. 2004; 5:282–295. [PubMed: 15071553]
40. Pezza RJ, Villarreal MA, Montich GG, Argarana CE. Vanadate inhibits the ATPase activity and DNA binding capability of bacterial MutS. A structural model for the vanadate-MutS interaction at the Walker A motif. Nucleic acids research. 2002; 30:4700–4708. [PubMed: 12409461]
41. Gambel AM, Desrosiers MG, Menick DR. Characterization of a P-type $Ca^{(2+)}$-ATPase from *Flavobacterium odoratum*. The Journal of biological chemistry. 1992; 267:15923–15931. [PubMed: 1386366]
42. Bhattacharyya P, Barnes EM Jr. ATP-dependent calcium transport in isolated membrane vesicles from *Azotobacter vinelandii*. The Journal of biological chemistry. 1976; 251:56–14-59. [PubMed: 9392]
43. Bers DM, Eisner DA, Valdivia HH. Sarcoplasmic reticulum $Ca^{2+}$ and heart failure - Roles of diastolic leak and $Ca^{2+}$ transport. Circulation Research. 2003; 93:487–490. [PubMed: 14500331]
44. Magyar CE, White KE, Rojas R, Apodaca G, Friedman PA. Plasma membrane $Ca^{2+}$-ATPase and NCX1 $Na^{+}/Ca^{2+}$ exchanger expression in distal convoluted tubule cells. American journal of physiology. Renal physiology. 2002; 283:F29–40. [PubMed: 12060584]
45. Budde CF, Mahan AE, Lu J, Rha C, Sinskey AJ. Roles of multiple acetoacetyl coenzyme A reductases in polyhydroxybutyrate biosynthesis in *Ralstonia eutropha* H16. Journal of bacteriology. 2010; 192:5319–5328. [PubMed: 20729355]
46. Booth IR, Edwards MD, Black S, Schumann U, Miller S. Mechanosensitive channels in bacteria: signs of closure? Nature reviews. Microbiology. 2007; 5:431–440.
47. Gode-Potratz CJ, Chodur DM, McCarter LL. Calcium and iron regulate swarming and type III secretion in *Vibrio parahaemolyticus*. Journal of bacteriology. 2010; 192:6025–6038. [PubMed: 20851895]
48. Sakai M, Futamata H, Kanazawa S. Effects of high concentrations of inorganic salts on swarming ability in fluorescent *Pseudomonas* strains. Bioscience Biotechnology and Biochemistry. 2003; 67:1479–1484.
49. Yeung AT, Torfs EC, Jamshidi F, Bains M, Wiegand I, Hancock RE, Overhage J. Swarming of *Pseudomonas aeruginosa* is controlled by a broad spectrum of transcriptional regulators, including MetR. Journal of bacteriology. 2009; 191:5592–5602. [PubMed: 19592586]
50. Ambudkar SV, Zlotnick GW, Rosen BP. Calcium efflux from *Escherichia coli*. Evidence for two systems. The Journal of biological chemistry. 1984; 259:6142–6146. [PubMed: 6373751]

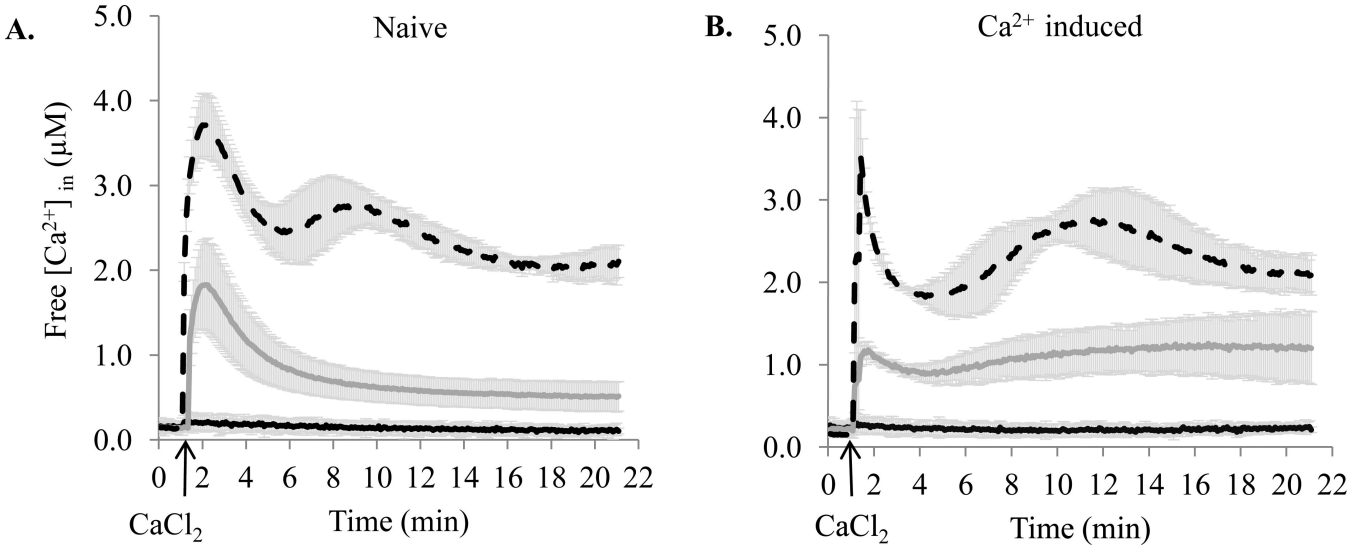


**Figure 1.**

The effect of externally added $Ca^{2+}$ on $[Ca^{2+}]_{in}$ in *P. aeruginosa* PAO1. Cells were grown in BMM with no added $Ca^{2+}$ (**A**) or in the presence of 5 mM $Ca^{2+}$ (**B**), and challenged with of 0 mM (black), 1mM (dark grey), and 5 mM (dash) $Ca^{2+}$. The basal level of luminescence was monitored for 1 min. 1 mM or 5 mM $CaCl_2$ was added at the time indicated by the arrow, followed by luminescence for 20 min. Changes in free $[Ca^{2+}]_{in}$ were calculated as described in the Methods section. The averages of at least three independent experiments are plotted.

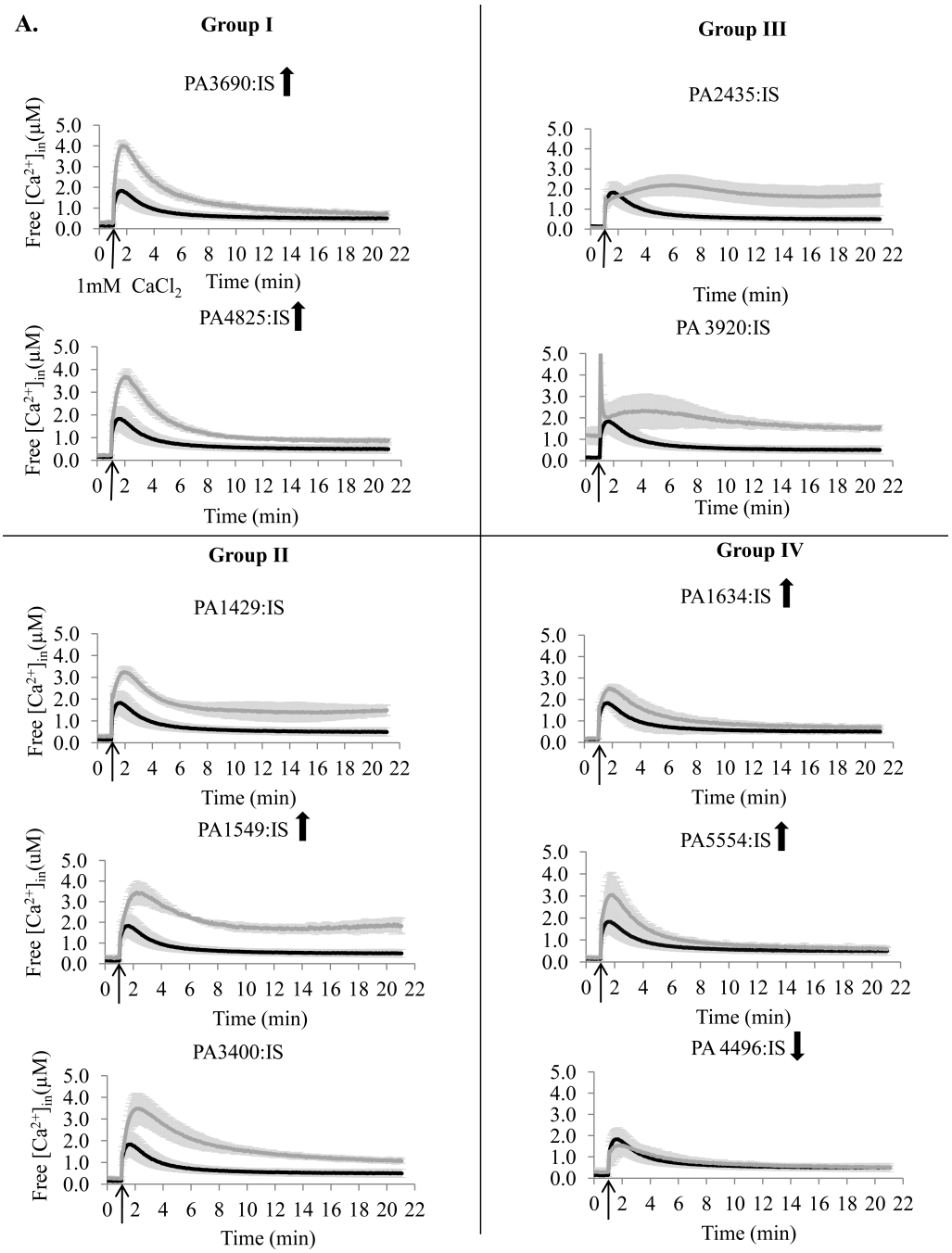

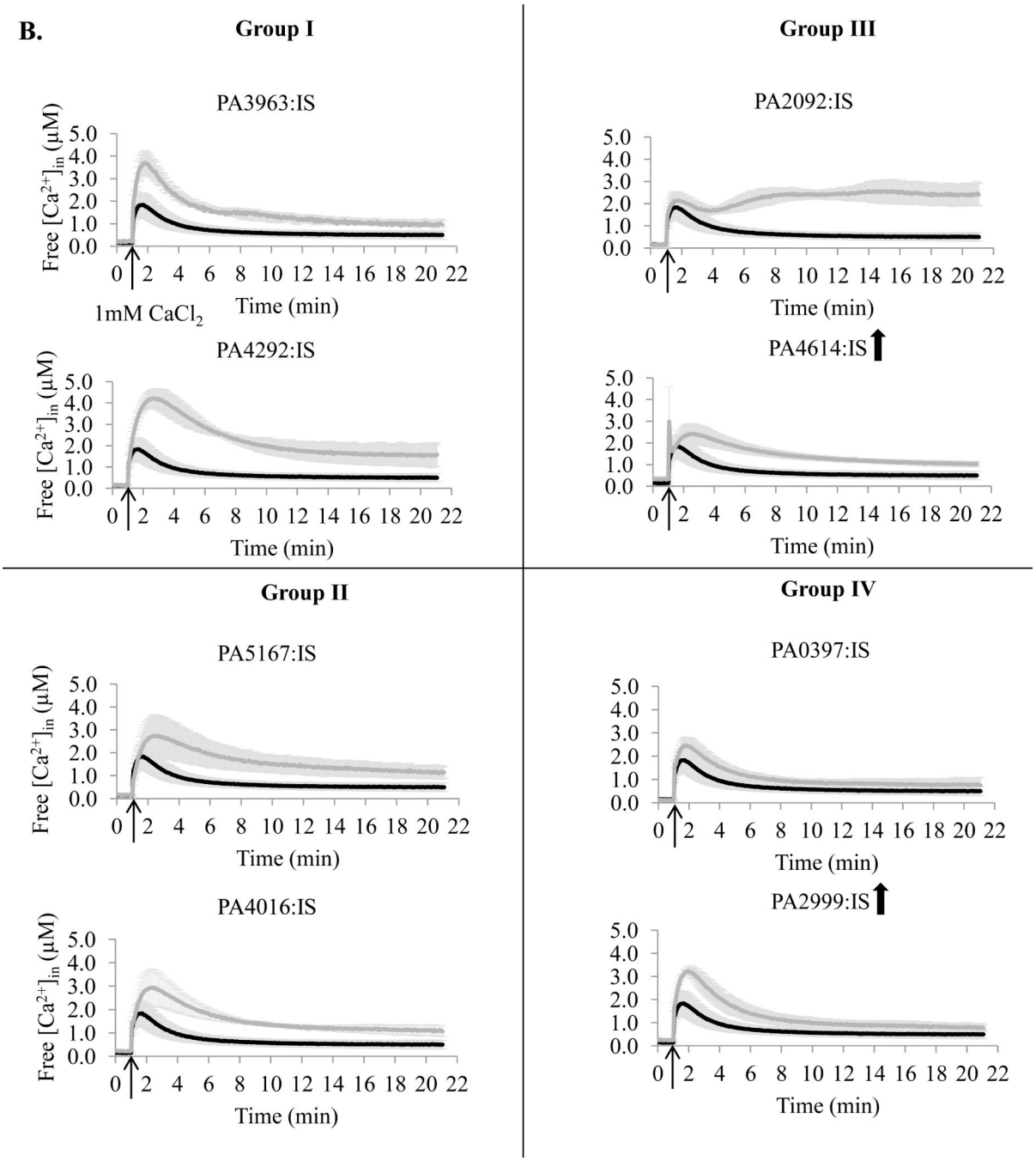


**Figure 2.**

Free $[Ca^{2+}]_{in}$ profiles of transposon mutants with disrupted ATP-dependent transporters (**A)** or ion exchange transporters (**B).** The mutants were obtained from the University of Washington Two - Allele library. Cells were grown in BMM media with no added $Ca^{2+}$. The basal level of luminescence was monitored for 1 min. 1 mM $CaCl_2$ was added at the time indicated by the arrow, followed by luminescence measurements for 20 min. Changes in free $[Ca^{2+}]_{in}$ were calculated as described in the Methods section. PA numbers represent the open reading frames in PAO1 genome. Black, PAO1 wild type; grey, transposon mutant.

The data is an average of at least three independent experiments. Upward and downward arrows indicate that the protein abundance was increased and decreased, correspondingly, during growth at 5 mM $CaCl_2$.

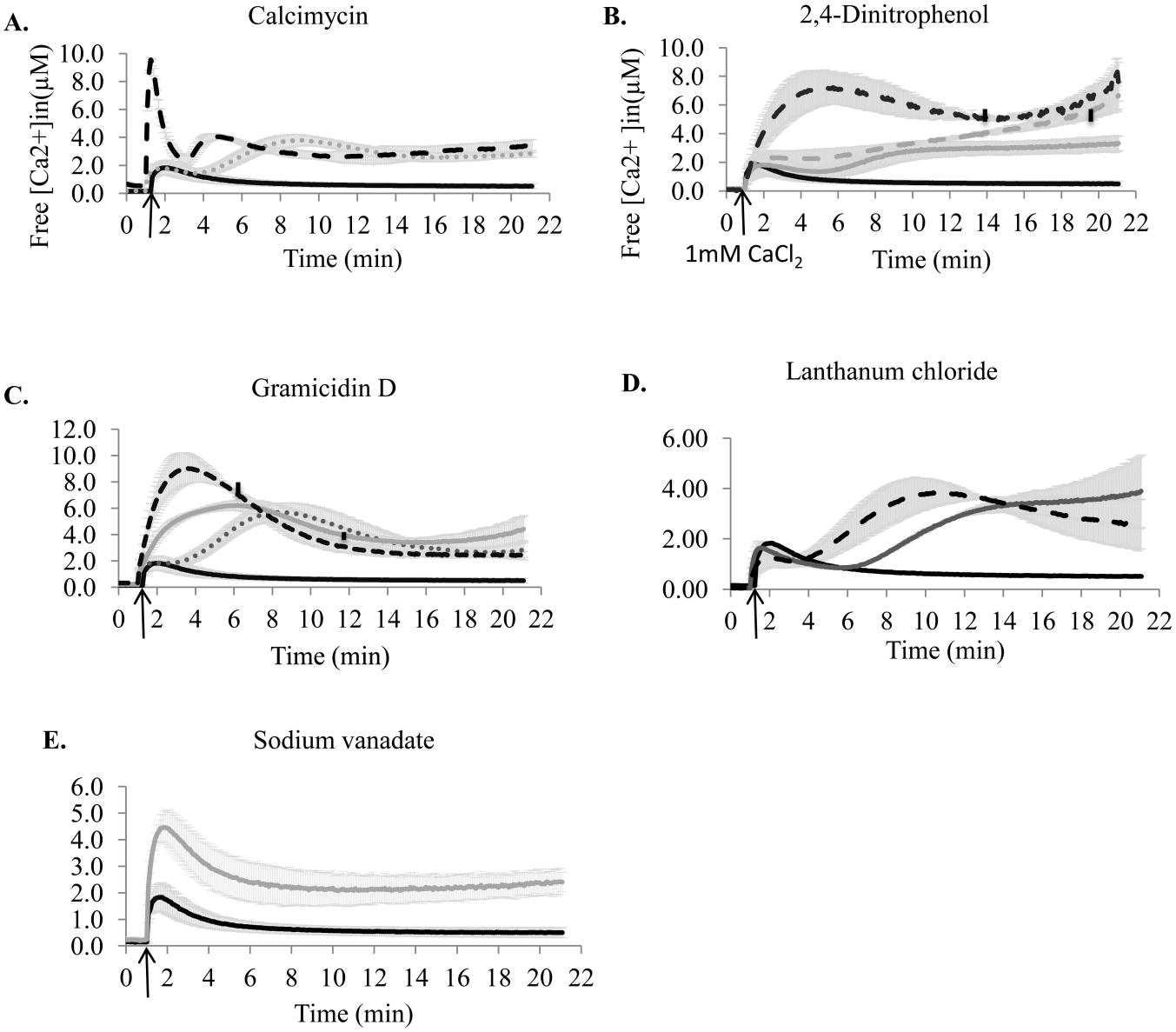


**Figure 3.**

Effect of inhibitors on free $[Ca^{2+}]_{in}$ in *P. aeruginosa* PAO1. Cells grown in BMM media containing no added $Ca^{2+}$ were treated with inhibitors for 10 min at room temperature. The basal level of luminescence was monitored for 1 min. 1 mM $CaCl_2$ was added at the time indicated by the arrow, followed by luminescence measurements for 20 min. Changes in free $[Ca^{2+}]_{in}$ were calculated as described in the Methods section. **A.** Calcimycin. Black, 0 mM; dashed black, 5 μM; small dotted grey, solvent control. **B.** Cells challenged with 2, 4 dinitrophenol. Black, 0mM; grey, 0.5 mM; dashed grey, 1 mM; dashed black, 2 mM. **C.** Gramicidin D. Black, 0 μg/ml; small dotted grey, 1 μg/ml; dashed black, 10 μg/ml; and grey, solvent control. Vertical lines on the plots indicate the points, at which the remaining available aequorin reached 10 % of the estimated total aequorin. **D.** $LaCl_3$. Black, 0 μM; grey, 300 μM, and dashed black, 600 μM. **E.** Vanadate (2 mM, pH 7.5). The data were averaged from at least three independent experiments.

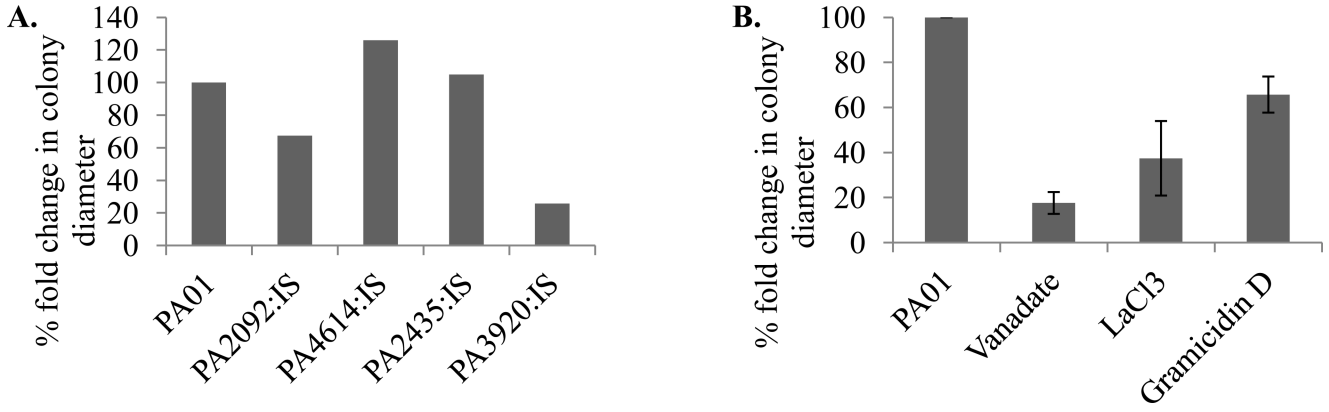


**Figure 4.**

Swarming motility. Cells were grown on swarming agar containing 0 mM or 5 mM $Ca^{2+}$. **A.** Group III mutants. **B.** PAO1 cells. Inhibitors: 2 mM vanadate, 600 μm $LaCl_3$, or 10 μg/ml gramicidin D were added to the medium prior to plating. Colony diameters were measured, and fold differences (5 mM *vs*. 0 mM) were calculated using the corresponding controls. The percentage of fold changes was calculated considering that the fold difference in untreated PAO1 was 100 %. The averages of at least three biological replicates were used to calculate the percentage of the fold changes. To avoid bias, in case of mutants, colony diameters were first averaged, and then the fold differences between the mutants and WT were calculated. The standard deviation between replicates was below 10 %.

**Table 1**

Protein prediction and identification. Transposon mutants.

| PA ORF[a] | Protein name, gene name[b] | Predicted domain(s)[c] | Best characterized hit in the nr NCBI, Accession #, Organism, % identity[d] | Transposon mutant PW#[e] Mutant Genotype | Mutant Designated Name |
|---|---|---|---|---|---|
| **ATP-driven transporters** | | | | | |
| PA1429 | Probable cation transporting P-Type ATPase | E1-E2 ATPase | P-type $Na^+$ ATPase, BAF91372.2, *Exiguobacterium aurantiacum*, 45% | PW3596 PA1429-E05::ISlacZ/hah | PA1429::IS |
| **PA4825** | Probable $Mg^{2+}$ transport ATPase, P-Type, *mgtA* | E1-E2 ATPase | $Ca^{2+}$/$Mn^{2+}$ P-type ATPase PMR1, CAB87245, *Candida albicans*, 25% | PW9116 PA4825-F12::ISphoA/hah | PA4825::IS |
| **PA3690** | Probable metal-transporting P-type ATPase | E1-E2 ATPase; Heavy metal associated domain | $Cd^{2+}$ /$Zn^{2+}$ transporting ATPase, HMA3 P0CW78.1, *Arabidopsis thaliana*, 32% | PW7241 PA3690-C04::ISlacZ/hah | PA3690::IS |
| **PA1634** | $K^+$-transporting ATPase, beta subunit, *kdpB* | E1-E2 ATPase | NA | PW3911 PA1634-E05::ISlacZ/hah | PA1634::IS |
| PA2435 | Heavy metal translocating P-type ATPase, *hmtA* | E1-E2 ATPase | | PW5099 PA2435-A02::ISphoA/hah | PA2435::IS |
| PA3920 | Probable metal transporting P-type ATPase | E1-E2 ATPase; Heavy-metal-associated domain | Cation transporting ATPase, NP_440588, 44%, *Synechocystis* PCC6803, 44% | PW7626 PA3920-G01::ISphoA/hah | PA3920::IS |
| PA1549 | Probable cation-transporting P-type ATPase | E1-E2 ATPase; Heavy-metal-associated domain | CtpA, AAW66130, *Rubrivivax gelatinosus*, 36% | PW3788 PA1549-G12::ISphoA/hah | PA1549::IS |
| **PA5554** | Probable ATPase synthase, beta subunit, *atpD* | F1 ATP synthase | F1F0-ATP synthase β subunit, Q587Q4, *Acidithiobacillus ferroxidans*, 77% | PW10412 PA5554-B01::ISlacZ/hah | PA5554::IS |
| PA4496 | Probable ABC transporter, substrate binding subunit | Substrate binding component | Dipeptide binding protein chain A, 1DPP A, *E. coli*, 50% | PW8565 PA4496-F02::ISphoA/hah | PA4496::IS |
| PA3400 | Hypothetical protein | ABC type transporter | NA | PW6735 PA3400-H11::ISphoA/hah | PA3400::IS |
| **Ion gradient driven exchangers** | | | | | |
| PA3963 | Probable Transporter | Cation Efflux Superfamily | Zinc transporter, YiiP, 3H90_A, *E.coli* K-12, 45% | PW7707 PA3963-E02::ISphoA/hah | PA3963::IS |
| PA2092 | Probable major facilitator superfamily transporter | Major Facilitator Superfamily | Purine efflux pump PbuE, Q0GQS6.1, *Bacillus amyloliquefaciens*, 35% | PW4602 PA2092-F01::ISlacZ/hah | PA2092::IS |
| PA4292 | Probable Phosphate transporter | $PO_4^{3-}$/$SO_4^{2-}$ permease | NA | PW8230 PA4292-A03::ISphoA/hah | PA4294::IS |

| PA ORF[a] | Protein name, gene name[b] | Predicted domain(s)[c] | Best characterized hit in the nr NCBI, Accession #, Organism, % identity[d] | Transposon mutant PW#[e] Mutant Genotype | Mutant Designated Name |
|---|---|---|---|---|---|
| PA0397 | Probable cation efflux system protein | Cation efflux family | Znt-like transporter 2, Q8NEW0.1, *Homo sapiens*, 27% | PW1733 PA0397-E03::ISlacZ/hah | PA0397::IS |
| **Other transporters** | | | | | |
| **PA2999** | Probable $Na^+$-translocating NADH:ubiquinone oxidoreductase subunit, *nqrA* | NADH-quinone reductase domain | $Na^+$ translocating NADH ubiquinone oxidoreductase subunit A , ZP_08756125.1, *Haemophilus pittmaniae* HK85,58% | PW6021 PA2999-D10::ISlacZ/hah | PA2999::IS |
| **PA4614** | Probable conductance mechanosensitive channel, *mscL* | Large-conductance mechanosensitive channel | Mechanosensitive channel large, MscL chain A, 3HZQ_A, *Staphylococcus aureus*, 36% | PW8772 PA4614-B11::ISphoA/hah | PA4614::IS |
| PA5167 | Dicarboxylic acid transporter, *dctP* | Bacterial extracellular solute binding | | PW9688 PA5167-F06::ISphoA/hah | PA5167::IS |
| PA4016 | Hypothetical protein | Membrane lipoprotein lipid attachment site | NA | PW7791 PA4016-E06::ISphoA/hah | PA4106::IS |

[f] Proteins were identified by using LC-MS/MS. Protein identification was accepted if the probability threshold was greater than 99% and at least three peptides were identified, each with 95% certainty. Spectral count (SC) was used to estimate the differential protein abundance. Fold difference was calculated as a ratio of the number of the peptides identified at 5 mM vs. 0 mM $Ca^{2+}$. ND, protein was detected at 0 mM and was not detected at 5 mM $Ca^{2+}$. New, protein was detected at 5 mM, but was not detected at 0 mM $Ca^{2+}$. PA number and fold difference (in brackets) are provided for the identified proteins that are encoded within the operonic gene clusters of the predicted proteins.

NA. No characterized hits with greater than 25% amino acid sequence identity were found.

[a] Gene identifier in the PAO1 genome available at www.pseudomonas.com.

[b] As annotated in the PAO1 genome.

[c] Domains were predicted by the algorithms in CDD and PROSITE.

[d] The % identity was calculated over the full length of the proteins using transporter proteins encoded in PAO1 genome as a query.

[e] The mutant strain identifier in the UW library of transposon mutants available at www.gs.washington.edu.